Gas-Phase Conformation of Biological Molecules: Bradykinin

Thomas Wyttenbach, Gert von Helden, and Michael T. Bowers*

*Contribution from the Department of Chemistry, University of California,
Santa Barbara, California 93106*

Received October 26, 1995. Revised Manuscript Received February 27, 1996[⊗]

Abstract: Several cationized forms of bradykinin (BK) were generated in the gas phase using matrix assisted laser desorption ionization (MALDI). Accurate collision cross sections were obtained using the ion chromatography method. The species studied include $(BK + H)^+$, $(BK + Na)^+$, and $(BK - H + 2Na)^+$. It was found that all three species had very similar cross sections of 245 ± 3 Å^2, and these cross sections were independent of temperature from 300 to 600 K. It could be concluded from these data that BK wraps itself around the charge center(s) in a globular shape whose time average size changes little up to 600 K. The arrival time distributions of all three systems were narrow, only slightly broader than expected for a single species indicating cationized BK exists in only a few low-energy conformers at low temperature. A detailed analysis of the data was done using molecular mechanics/dynamics of the AMBER 4.0 suite of programs. The calculations were in excellent agreement with experiment in that scatter plots indicated cross sections of 100 member structural sets of $(BK + H)^+$, $(BK + Na)^+$, and $(BK - H + 2Na)^+$ were very similar. Further, very extensive dynamics studies over the range 200 to 600 K indicated the lowest energy conformers exhibited cross sections independent of temperature in agreement with experiment and supported the indication that only a few conformers are involved. The absolute magnitudes of the AMBER generated 0 K structures were ∼10% smaller than experiment. The discrepancy decreased to ∼5% when the systems were thermally averaged at 300 K. Selected 0 K conformers of $(BK + H)^+$ were calculated using AM1 and PM3 from AMBER starting structures. It was found that the 0 K cross sections increased by ∼5% over the AMBER structures providing better agreement with experiment. The extensive conformer sets generated in the scatter plots were analyzed to see which parts of BK preferred to bind to the charge sites. As expected the binding was global, but each isomer or system had different preferred binding sites. We looked for a preference of BK forming a β-turn in the Ser^6-Pro^7-Phe^8-Arg^9 sequence since such a feature had been proposed in solution NMR studies. We found little evidence for β-turns in our 500 conformers of variously cationized BK in the gas phase.

Introduction

It is axiomatic in biochemistry that structure and function are intimately related. As a consequence the quest for structures of biochemically interesting molecules has a long and rich history.[1] The concept of "structure" has many levels, from the most basic "connectivity" level (primary structure) that reveals how the atoms are connected to each other, to the subtleties that define actual conformations (secondary and tertiary structures). Connectivities are often determined by sequentially breaking off selected pieces of a molecule and analyzing either what departed or what is left. In this regard, the powerful new methods of mass spectrometry have become most revealing.[2] Conformational information on biomolecules, on the other hand, has relied almost exclusively on X-ray analysis of crystals of molecules of known connectivity,[3] although recently multiple-pulse NMR methods have been useful in obtaining conformational information on smaller biomolecules in solution.[4]

In the last several years mass spectrometry has begun to address the question of molecular conformation of complex molecules. Technological breakthroughs have made it possible to "vaporize" intact molecules or molecular assemblies into the gas phase with little or no structural disruption. While fast atom bombardment (FAB)[5] led the way over a decade ago, it is the emergence of matrix assisted laser desorption ionization (MALDI)[6] and electrospray ionization (ESI)[7] that have really opened up the large molecule field to mass spectrometric analysis.

Electrospray allows direct sampling of ions from solution and has stimulated tremendous interest in the mass spectrometry community. While most structural applications are directed to sequence determination[8] (primary structure), interest in developing methods directed toward conformational analysis is beginning to appear. For example, deuterium exchange studies both in solution[9] and in the gas phase[10] have been used to probe the number of exchangeable hydrogens, results that allow estimates to be made of the degree of folding of targeted proteins. Collisional methods in triple quadrupole instruments have been used to estimate ion collision cross sections and how these change with charge state.[11,12] Work is proceeding on the critical

(5) Monagham. J. J.; Barber, M.; Bordolim, R.; Sedgewick, E.; Taylor, A. *Org. Mass Spectrom.* **1982**, *18*, 25; *17*, 596.

(6) Hillenkamp, F.; Karas, M.; Beavis, R. C.; Chait, B. T. *Anal. Chem.* **1991**, *63*, 1193A.

(7) Fenn, J. B.; Mann, N.; Meng, C. K.; Wong, S. F. *Mass Spectrom. Rev.* **1990**, *9*, 37.

(8) See, for example, Chait, B. K.; Wong, R.; Beavis, R. C.; Kent, S. B. H. *Science* **1993**, *262*, 89. Bieman, K. *Fresenius' Z. Anal. Chem.* **1992**, *343*, N1:25; *Annu. Rev. Biochem.* **1992**, *61*, 977.

(9) Katta, V.; Chait, B. T. *Rapid Commun. Mass Spectrom.* **1991**, *5*, 214; *J. Am. Chem. Soc.* **1993**, *115*, 6317.

(10) Winger, B. E.; Light-Wahl, K. J.; Rockwood, A. L.; Smith, R. D. *J. Am. Chem. Soc.* **1992**, *114*, 5897. Wood, T. D.; Chorush, R. A.; Wampler, F. M., III; Little, D. P.; O'Connor, P.B.; McLafferty, F. W. *Proc. Natl. Acad. Sci. U.S.A.* **1995**, *92*, 2451. Suckaw, D.; Shi, Y.; Beu, S. C.; Senko, M. W.; Quinn, J. P.; Wampler, F. M.; McLafferty, F. W. *Proc. Natl. Acad. Sci. U.S.A.* **1993**, *90*, 790.

(11) Covey, T.; Douglas, D. J. *J. Am. Soc. Mass Spectrom.* **1993**, *4*, 616.

⊗ Abstract published in *Advance ACS Abstracts,* August 15, 1996.

(1) See, for example: Creighton, T. E. *Proteins; Structures and Molecular Properties,* 2nd ed.; W. H. Freeman: New York, 1993.

(2) For several issues devoted entirely to modern methods in mass spectrometry see: *Int. J. Mass Spectrom. Ion Proc.* **1991**, *111*, 1ff. *J. Am. Soc. Mass Spectrom.* **1993**, *4*, issues 7 an 8. *Acc. Chem. Res.* **1994**, *27*, issue 11.

(3) Diffraction Methods for Biological Macromolecules. *Methods Enzymal.* **1985**, *114* and *115*, 1ff and references therein.

(4) Dyson, H. J.; Wright, P. E. *Annu. Rev. Biophys. Chem.* **1991**, *20*, 519. Braun, W. *Q. Rev. Biophys.* **1987**, *19*, 115 and references therein.

question of whether ESI generated gas phase macromolecules and association complexes directly reflect properties of their solution precursors.[13,14] Very recently mobility methods have been used to probe conformations of cytachrome C[15] and several other biopolymers,[16] generated by a variety of ESI techniques, studies which also address the dual questions of ion conformation and correspondence to solution structure.

Because experimental information on conformations of biological molecules is so hard to obtain, theoretical methods have taken on heightened importance. Full ab initio procedures are impractical, but semiemperical[17,18] and especially molecular mechanics methods[19,20] have emerged as essential tools for estimating structures.[21-23] Molecular mechanics has the added advantage of allowing thermal averaging, or annealing studies, through use of the molecular dynamics aspects of these programs. What is needed are prototypical systems against which these methods can be calibrated. Traditional spectroscopic methods are useful for conformational studies on small molecules but have been applied only to the simplest biologically interesting species.[24] Hence charge distributions and geometries are usually parametrized by comparison with ab initio results on model systems.

In the past several years our group has developed mobility based methods[25] that allow determination of conformations of gas phase ions. These methods have been extremely successful for smaller rigid systems like carbon clusters[26] and metal carbon composites,[27] where theoretical candidate structures could be readily generated using standard quantum chemical methods. Since different geometric isomers of the same chemical makeup could often be separated in time and space using the technique, the name ion chromatography (IC) was coined.[28]

In the past year or so applications have been made to much more flexible "floppy" molecules like polyethylene glycol (PEG)

polymers[29] and crown ethers.[30] These applications required the use of molecular mechanics for generating candidate structures, and significant effort has been put into method development.[31] Consequently, it was decided it was time to try IC on a true biologically interesting molecule. Our choice is bradykinin, a small important polypeptide with the sequence Arg-Pro-Pro-Gly-Phe-Ser-Pro-Phe-Arg. We chose bradykinin not only because of its importance in the body's response to trauma[32] but because it has been extensively studied using both mass spectrometry in the gas phase[33,34] and a variety of other techniques in solution.[35,36] We are interested in comparing our results with those available in solution and commenting on any similarities of differences. This study will also provide an opportunity to use and evaluate the utility of molecular mechanics methods for extracting structural information consistent with the data and evaluate the parametrization of the methods themselves. Our findings follow.

Experimental Section

The ion chromatography technique has at its heart a cell where the ion under investigation undergoes thousands to millions of collisions with He atoms while being mildly accelerated in a weak electric field. As such it builds on well established mobility methods developed long ago by McDaniel and others[37] and has some parallels to an analytical device usually termed ion mobility spectrometry.[38-40] The IC method distinguishes itself by the wide variety of sources possible for ion injection and the high degree of theoretical analysis used to identify likely conformations of the target molecular ion. Sources used to date include electron ionization,[41] surface ionization,[42] discharge ionization,[43] laser desorption,[26,27,44] ESI,[15,16] and the source used for the present work, MALDI.[29,31]

Details of the source design have been given previously[31] as has the overall instrument configuration and operation.[45] In this work a small amount of bradykinin (BK), ~0.1%, was dissolved in a water/methanol solvent along with a large excess of 2,5-dihydroxybenzoic acid, ~99.9%. The solution was evaporated onto a rotating/translating sample holder. An excimer laser run as a nitrogen laser at ~50 Hz yielded a strong MALDI signal of protonated BK. When a large excess of NaI was added (~1%) the $(BK + H)^+$ signal was augmented by $(BK + Na)^+$ and $(BK - H + 2Na)^+$ signals. The ions were accelerated to 5 kV, mass selected, decelerated to a few eV (1 to 5 eV), and injected into the IC cell containing 3 Torr of He, where they drifted under the

(12) Cox, K. A.; Julian, R. K.; Cooks, R. G.; Kaiser, R. E. *J. Am. Soc. Mass Spectrom.* **1994**, *5*, 127.

(13) Ganem, B.; Li, Y-T.; Henion, J. D. *J. Am. Chem. Soc.* **1991**, *113*, 6294. Ganem, B.; Henion J. D. *Chemtracts: Org. Chem.* **1993**, *6*, 1.

(14) Cheng, X.; Chevy, R.; Bruce, J. E.; Schwartz, B. L.; Anderson, G. A.; Hofstadler, S. A.; Gale, D. C.; Smith, R. D.; Gao, J.; Sigal, G. B.; Mammen, M.; Whitesides, G. M. *J. Am. Chem. Soc.* **1995**, *117*, 8859.

(15) Clemmer, D. E.; Hudgins, R. R.; Jarrold, M. F. *J. Am. Chem. Soc.* **1995**, *117*, 10141.

(16) Jarrold, M. Private communication.

(17) Dewar, M. J. S.; Zoebisch, E. G.; Healy, E. F.; Stewart, J. J. P. *J. Am. Chem. Soc.* **1985**, *107*, 3902. Dewar, M. J. S.; Dieter, K. M. *J. Am. Chem. Soc.* **1986**, *108*, 8075.

(18) Stewart, J. J. P. *J. Comput. Chem.* **1989**, *10*, 209, 221.

(19) See, for example: Weiner, P. K.; Kollman, P. A. *J. Comput. Chem.* **1981**, *2*, 287 and references therein.

(20) Hopfinger, A. J.; Pearlstein, R. A. *J. Comput. Chem.* **1981**, *5*, 486 and references therein.

(21) Kollman, P. A.; Merz, K. M. *Acc. Chem. Res.* **1990**, *23*, 246 and references therein.

(22) Vangunsteren, W. F.; Luque, F. J.; Timms, D.; Torda, A. E. *Annu. Rev. Biophys. Biomol. Struct.* **1994**, *23*, 847 and references therein.

(23) Malhotra, A.; Tan. R. K. Z.; Harvey, S. C. *Biophys. J.* **1994**, *66*, 1777 and references therein.

(24) See, for example: Brown, R. D.; Godfrey, P. D.; Storey, J. W. V.; Bassez, M. P. *J. Chem. Soc., Chem. Commun.* **1978**, *547*. Suenram, R. D.; Lovas, F. J. *J. Mol. Spectrosc.* **1978**, *72*, 372. Schäfer, L.; Sellers, H. L.; Lovas, F. J.; Suenram, R. D. *J. Am. Chem. Soc.* **1980**, *102*, 6566.

(25) Kemper, P. R.; Bowers, M. T. *J. Phys. Chem.* **1991**, *95*, 5134.

(26) von Helden, G.; Hsu, M-T.; Gotts, N. G.; Bowers, M. T. *J. Phys. Chem.* **1993**, *97*, 8182. von Helden, G.; Hsu, M-T.; Kemper, P. R.; Bowers, M. T. *J. Chem. Phys.* **1991**, *95*, 3835. von Helden, G.; Kemper, P. R.; Gotts, N. G.; Bowers, M. T. *Science* **1993**, *259*, 1300. Gotts, N. G.; von Helden, G.; Bowers, M. T. *Int. J. Mass Spectrom. Ion Proc.* **1995**, *149/150*, 217.

(27) von Helden, G.; Gotts, N. G.; Maitre, P.; Bowers, M. T. *Chem. Phys. Lett.* **1994**, *227*, 601. Bowers, M. T. *Acc. Chem. Res.* **1994**, *27*, 234. Lee, S.; Gotts, N. G.; von Helden, G.; Bowers, M. T. *Science* **1995**, *267*, 999.

(28) Bowers, M. T.; Kemper, P. R.; von Helden, G.; van Koppen, P. A. M. *Science* **1983**, 1446.

(29) von Helden, T.; Wyttenbach, T.; Bowers, M. T. *Science* **1995**, *267*, 1483.

(30) Lee, S.; Wyttenbach, T. von Helden, G.; Bowers, M. T. *J. Am. Chem. Soc.* **1995**, *117*, 10159.

(31) von Helden, G.; Wyttenbach, T.; Bowers, M. T. *Int. J. Mass Spectrom. Ion Proc.* **1995**, *146/147*, 349.

(32) Regoli, D.; Barabe, J. *Pharmacol. Rev.* **1980**, *32*, 1.

(33) Thorne, G. C.; Ballard, K. D.; Gaskell, S. J. *J. Am. Soc. Mass Spectrom.* **1990**, *1*, 238.

(34) Burk, D. M. Macfarlane, R. D. *J. Am. Soc. Mass Spectrom.* **1991**, *2*, 379; *Int. J. Mass Spectrom. Ion Proc.* **1991**, *111*, 55.

(35) Cann, J. R.; Vatter, A.; Vovrek, R. J.; Stewart, J. M. *Peptides* **1986**, *7*, 1121; Cann, J. R.; London, R. E.; Unkefer, C. J.; Vovrek, R. J.; Stewart, J. M. *Int. J. Peptide Protein Res.* **1987**, *29*, 486 and references therein.

(36) Lee, S. C.; Russell, A. F.; Laidig, W. D. *Int. J. Peptide Protein Res.* **1990**, *35*, 367 and references therein.

(37) Mason, E. A.; McDaniel, E. W. *Transport Properties of Ions in Gases*; Wiley: New York, 1988.

(38) Hill, H. H., Jr.; Siems, W. F.; St. Louis, R. H.; McMinn, D. G. *Anal. Chem.* **1990**, *62*, 1201. St. Louis, R. H.; Hill, H. H. *Crit. Rev. Anal. Chem.* **1990**, *21*, 321 and references therein.

(39) Eiceman, G. A. *Crit. Rev. Anal. Chem.* **1991**, *22*, 17 and references therein.

(40) Karpas, Z. *Forensic Sci. Rev.* **1990**, *1*, 103 and references therein.

(41) van Koppen, P. A. M.; Kemper, P. K.; Bowers, M. T. *J. Am. Chem. Soc.* **1992**, *114*, 1083.

(42) van Koppen, P. A. M.; Kemper, P. R.; Bowers, M. T. *J. Am. Chem. Soc.* **1992**, *114*, 10941.

(43) Weis, P.; Kemper, P. R.; Bushnell, J.; Bowers, M. T. To be published.

(44) Shelminov, K. B.; Hunter, J. M.; Jarrold, M. F. *Int. J. Mass Spectrom. Ion Proc.* **1994**, *138*, 17.

(45) Kemper, P. R.; Bowers, M. T. *J. Am. Soc. Mass Spectrom.* **1990**, *1*, 197.

influence of a weak electric field. The pulse of ions entering the cell was "clipped" to ~5 μs width using an electronic gate, allowing an arrival time distribution (ATD) to be measured for the ions exiting the cell once they had passed through a quadrupole mass filter. The cell temperature could be varied from 80 to 600 K.

Data Analysis. The usual way to characterize ions drifting through He gas at velocity v_D under the influence of a weak electric field E is by the relationship

$$v_D = KE \tag{1}$$

where the proportionality constant K is termed the mobility. At standard temperature and pressure kinetic theory indicates[37]

$$K_0 = \frac{3q}{16N_o}\left[\frac{2\pi}{k_b T}\right]^{1/2}\left[\frac{1}{\mu^{1/2}\Omega^{(1,1)}}\right] \tag{2}$$

where q is the ion charge, N_o the He number density at STP, T the temperature, μ the ion−He reduced mass, and $\Omega^{(1,1)}$ the collision integral. When the collision between the ion and He gas can be approximated by a hard sphere potential then

$$\Omega^{(1,1)}_{HS} = Q_{HS} = \pi r^2_{HS} \tag{3}$$

where Q_{HS} is the hard sphere cross section and r_{HS} is one-half the distance between the center of mass of the ion and the He nucleus at the point of contact. Under these conditions it is clear from eqs 2 and 3 that the reduced mobility, K_o, is proportional to $(Q_{HS})^{-1}$ for a fixed value of T. Hence, accurate measurement of K_o, which is straightforward using our arrival time data, yields an accurate experimental measurement of the 3-dimensional collision cross section. These data can be directly compared to predictions of model structures as described in the next section. This level of analysis has proved satisfactory for carbon clusters[26,44] and other systems[27,30] at temperatures near and above 300 K. However, in our extensive studies of PEG polymers[31] over a wide temperature range (80 to 550 K) we observed that the hard sphere model was inadequate at low temperatures ($T \leq 200$ K). Hence, a more sophisticated model of the collision was required. We chose to use the potential of the form

$$V(r) = \frac{n\epsilon}{n(3+\gamma)-12(1+\gamma)}\left[\frac{12}{n}(1+\gamma)\left(\frac{r_m}{r}\right)^n - 4\gamma\left(\frac{r_m}{r}\right)^6 - 3(1-\gamma)\left(\frac{r_m}{r}\right)^4\right] \tag{4}$$

where ϵ is the well depth at the equilibrium distance r_m between the ion and He, n is the repulsive exponent, and γ is a term that ranges between 0 and 1 expressing the relative importance of the r^{-6} and r^{-4} terms. Because the ions of interest here are quite complex (BK has a total of 150 atoms) it is not possible to determine the collision integral exactly. However, as previously discussed, we can use eq 4 in a pairwise fashion between each atomic center on the ion and the He atom yielding an "effective" radius $r_{eff,i}$ between He and atom i. These effective radii are then used to calculate collision cross sections using the Monte Carlo techniques we have developed for this purpose.[26]

Theoretical Methods. The experimental data yield accurate values of the mobility that can be transformed into accurate 3-dimensional cross sections as already described. In order to extract conformational information from these data, our approach has been to use model structures to generate cross sections for comparison. From the beginning we have decided to use model structures generated from the best available theoretical methods using no additional approximations beyond those embodied in the theory. For carbon clusters[26] semiempirical PM3 methods[18] were used and found to give very reliable structures. These methods cannot be easily adapted for larger systems, however, and hence for our work on Na$^+$ cationized PEG polymers[29,31] and alkali ion/18-crown-6 complexes[30] we used molecular mechanics methods to obtain candidate structures.

The problem in finding global minimum structures for large molecules is twofold. First, their sheer size makes even semiempirical calculations formidable. BK, for instance, has 150 atoms and 40 bonds capable of torsional motion due to low barriers. It is this latter feature that makes use of molecular mechanics mandatory. Due to the many torsions, literally millions of local minima are generated in BK. Hence, the odds are very high that structures generated by semiempirical methods will become trapped in a local minimum remote from the global minimum.

One way to overcome this is to use molecular mechanics to do selective annealing studies to generate a representative cohort of structures having lower energy configurations. In our case we used the AMBER 4.0 suite of programs[46] installed on an IBM RISC system 6000 workstation. As a consequence of the nature of the computer system available, a compromise between computation time and quality of results had to be struck. Based on the earlier work on BK[47] and on preliminary results on glycine polymers in our own lab[48] we found the following procedure to be satisfactory. First, molecular dynamics was carried out at 800 K for 30 ps followed by gradual reduction to 100 K over 10 ps of additional dynamics. The resultant structure was energy minimized to form a 0 K structure, and stored. This structure was then used as the starting point for another 800 K annealing run, etc. One hundred 0 K structures were generated using this technique for each of the BK cationized systems considered. In our experience this process will adequately access the lower energy portion of the potential hypersurface and will hopefully include structures close to those observed in experiment.

The AMBER suite of programs allow study of the thermal energy motion of BK over the temperature range 80−600 K. For each of the BK systems studied we did long molecular dynamics runs. These runs started with the lowest energy 0 K structure found by the annealing process described above and were initiated with a run at 600 K lasting 1 ns with a structure saved every 500 fs. The terminal 600 K structure was then used to initiate a similar run at 500 K and so on to 200 K. Except for one special case discussed later, 200 K was the lowest temperature sampled using this dynamics procedure. In all 10 000 structures are generated across the 200 to 600 K temperature range for each of the five BK systems studied experimentally. This protocol was successful in describing the temperature dependence for the PEG polymer systems.[31]

In order to calculate 3-dimensional cross sections from the structures obtained, we used the Monte Carlo methods described previously.[26] Based on our experience with PEG polymers we chose to use the interaction potential given in eq 4 and the values of ϵ and r_m from the MM3 compilation.[49] A more detailed description of the process is given elsewhere.[31] The 50 000 cross section calculations necessary for the temperature-dependence studies were done on a 400 node SP2 machine at the Department of Defense Maui Computer Center.

For all of the AMBER calculations we used the all atom force field[50] but froze all bonds involving hydrogen atoms using the SHAKE algorithm.[51] For a small selection of the three protonated versions of BK we augmented the AMBER studies using AM1[17] and PM3[18] semiempirical calculations as supplied in the GAMESS software package.[52] The selected AMBER 0 K structures were used as starting points and new energy minimizations were done using AM1 and PM3.

Results

1. Experiment. A MALDI mass spectrum obtained when a trace of BK is dissolved in a DHB matrix is given in Figure 1a. The base peak in the spectrum is (BK + H)$^+$ at *m/z* 1061 with a number of weak fragment peaks observed as well as

(46) Pearlman, D. A.; Case, D. A.; Caldwell, J. C.; Seibel, G. L.; Singh, U. C.; Weiner, P.; Kollman, P. A. *AMBER 4.0*, University of California, San Francisco, 1991.

(47) Salvino, J. M.; Seoane, P. R.; Dolle, R. E. *J. Comput. Chem.* **1993**, *14*, 438.

(48) Wyttenbach, T.; Bowers, M. T. To be published.

(49) Allinger, N. L.; Zhou, X.; Bergsma, J. *J. Mol. Struct. (Theochem)* **1994**, *312*, 69.

(50) Weiner, S. J.; Kollman, P. A.; Nguyen, D. T.; Case, D. A. *J. Comput. Chem.* **1986**, *7*, 230.

(51) Ryckaert, J. P.; Ciccotti, C.; Berendsen, H. J. C. *J. Comput. Phys.* **1977**, *23*, 327.

(52) Schmidt, M. W.; Baldridge, K. K.; Boatz, J. A.; Jensen, J. H.; Koseki, S.; Gordon, M. S.; Nguyen, K. A.; Windus, T. L.; Elbert, S. T. *QCEP Bull.* **1990**, *10*, 52.
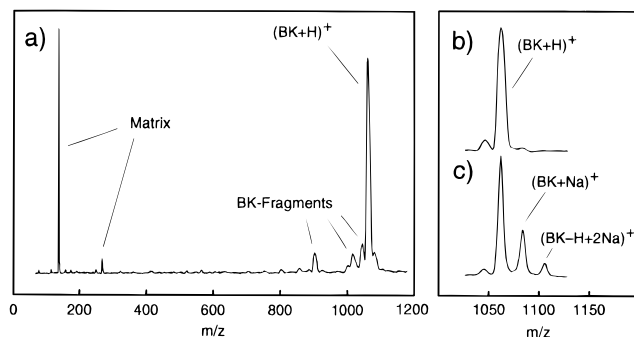
Figure 1. MALDI mass spectra of bradykinin in a 2,5-dihydroxyben-zoic acid matrix: (a) 0.1% BK in DBA; (b) blowup of the region around *m/z* 1060 of spectra in part a; (c) spectra when 1% NaI is added to the mixture in part a.
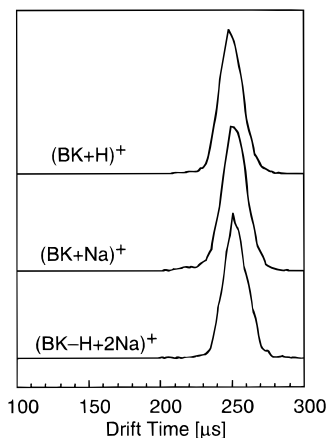

Figure 2. Arrival time distributions for the three cationized forms of BK shown in Figure 1c. Note the arrival times and peak widths are essentially identical for the three species. The temperature was 300 K.

matrix peaks at low mass. Of interest is the fact that no (BK + 2H)$^{2+}$ ions are observed at *m/z* 531 in spite of the fact that BK has argenine residues at both the N- and C-terminal positions. Many attempts were made to observe the (BK + 2H)$^{2+}$ ion using a wide range of experimental conditions, but none were successful. Arginine (ARG) has the highest proton affinity of the 20 common amino acids[53] due to the presence of the highly basic guanidine side chain. In solution it is routinely assumed all ARG residues are protonated. Since the two ARG residues in BK are at opposite ends of the molecule it was thought protonation of both in the MALDI experiment might occur. That it does not strongly suggests protonation occurs in the gas phase rather than in the matrix/BK solid solution.

Part b of Figure 1 shows a blowup of the region near *m/z* 1061. The small peak at 22 *m/z* units above (BK + H)$^+$ is due to (BK + Na)$^+$ where the Na$^+$ ions are either leached from the glassware in sample handling or present as impurities in the BK or DHB samples. When NaI is added to the matrix (at ~1% abundance) the (BK + Na)$^+$ peak is strongly enhanced as shown in Figure 1c. Of interest is the fact that a substantial (BK − H + 2Na)$^+$ peak is also present, a feature sometimes observed with other peptides.[54]

The arrival time distributions (ATD's) observed for (BK + H)$^+$, (BK + Na)$^+$, and (BK − H + 2Na)$^+$ are given in Figure 2. These three ATD's were obtained under identical experimental conditions. The centers of the distributions "arrive" at

(53) (a) Gorman, G. S.; Speir, P. J.; Turner, C. A.; Amster, I. J. *J. Am. Chem. Soc.* **1992**, *114*, 3986. (b) Wu, Z.; Fenselau, C. *Rapid Commun. Mass Spectrom.* **1992**, *6*, 403.
(54) See, for example: Grese, R. P.; Cerny, R. L.; Gross, M. L. *J. Am. Chem. Soc.* **1989**, *111*, 2835.
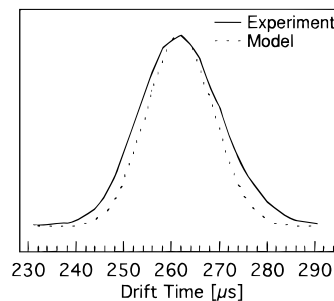

Figure 3. A blowup of the arrival time distribution of (BK + H)$^+$ from Figure 2 given as the solid line. The dotted line is the peak shape expected for transport of a single conformer through the drift cell assuming a mobility appropriate for the center of the experimental ATD.
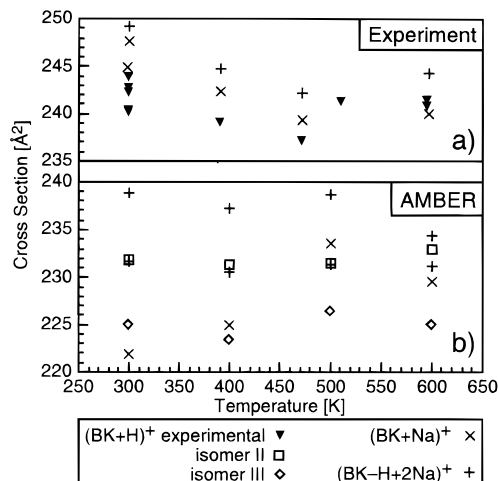

Figure 4. A plot of the cross section of cationized BK versus temperature: (a) experimental data for (BK + H)$^+$ (▼); (BK + Na)$^+$ (×), and (BK − H + 2Na)$^+$ (+); (b) thermally averaged molecular mechanics cross sections for isomers **II** and **III** of (BK + H)$^+$ (□ and ◇), (BK + Na)$^+$ (×), and (BK − H + 2Na)$^+$ (+).

nearly identical times at the detector indicating the mobilities and collision cross sections of all three are nearly identical [at 300 K the cross sections are 242 ± 5, 245 ± 5, and 247 ± 5 Å^2 for (BK + H)$^+$, (BK + Na)$^+$, and (BK − H + 2Na)$^+$, respectively]. Further, all three peaks are narrow and show no apparent structure eliminating the presence of stable conformers with modestly different structures. Similar results were observed for all temperatures between 80 and 580 K. This is a somewhat surprising result, especially the fact the sodiated BK ions have nearly the same cross sections as the protonated ions even though the nature of the bonding between the ionic site and the peptide must be substantially different.

In Figure 3 the experimental ATD for (BK + H)$^+$ at 300 K is compared with the exact solution of the ion transport equations for an ion with a single structure.[37] It is apparent that the experimental peak is somewhat broader than expected from the transport equations. This point will be discussed later.

The temperature dependence of the experimental cross sections for the three cationized forms of BK is given in Figure 4a. While some scatter does occur (about ±1%), it is clear that all three cross sections are essentially independent of *T* between 300 and 600 K. By comparison, a fairly strong temperature dependence was observed in the PEG polymers, and this dependence increased with size.[31] For example, the cross section of Na$^+$PEG9 increased by ~1% between 300 and 600 K, Na$^+$PEG13 increased ~4%, and Na$^+$PEG17 increased ~6%. Analysis of the molecular modeling for these systems, which agreed very well with experiment, indicated the part of
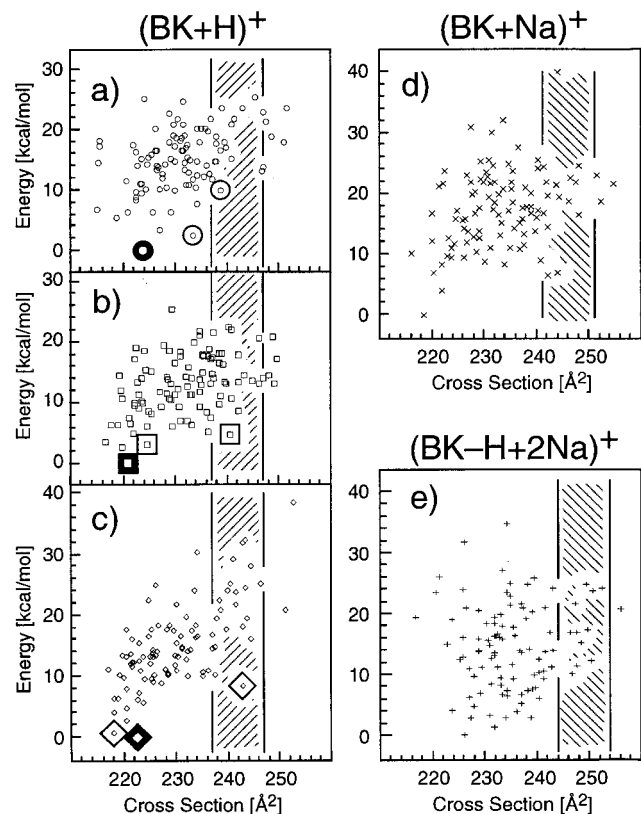
Figure 5. Scatter plots of relative energy versus cross section generated by annealing molecular dynamics (see text). Isomers **I**, **II**, and **III** of (BK + H)$^+$ are given in parts a, b, and c, respectively, (BK + Na)$^+$ in part d, and (BK − H + 2Na)$^+$ in part e. The cross hatched vertical box is the range of observed experimental cross sections. The highlighted symbols in a−c were selected for semiemperical calculations using AM1 and PM3 (see Figure 8).
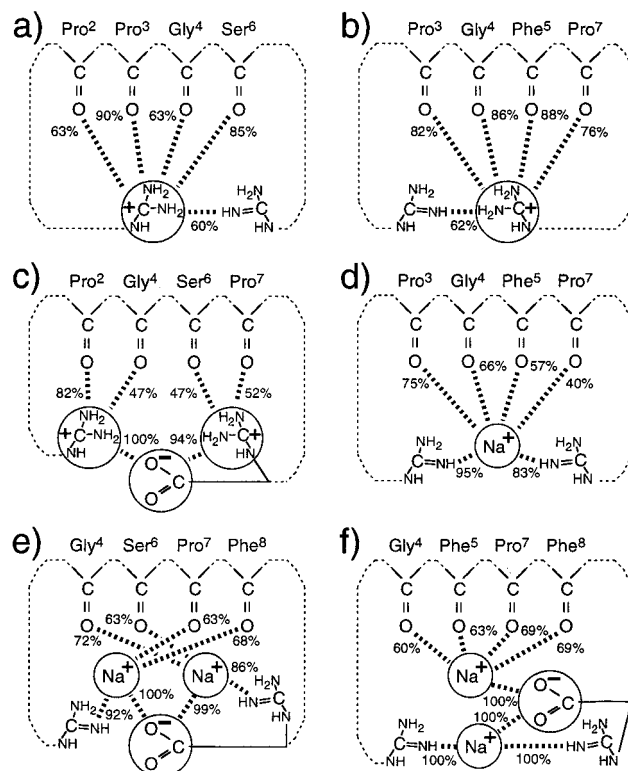

Figure 6. Schematic plots showing the most common electrostatic bonds between the charge center and various electronegative sites on BK. The data were obtained from analysis of the detailed structures of the scatter plots in Figure 5. The charge sites are circled for ease of identification. Parts a, b, and c are for isomers **I**, **II**, and **III** of (BK + H)$^+$, part d is for (BK + Na)$^+$, parts e and f are for the two separate conformer groups of (BK − H + 2Na)$^+$ (see text).

the polymer in direct contact with the Na$^+$ ion changed relatively little from 300 to 600 K, but the remote parts became "larger" on time average due to greater motion as T increased. Since no temperature dependence is observed in the BK systems, the implication is that essentially the entire BK molecule is held in place by the charge site allowing no time average expansion between 300 and 600 K.

2. Calculated Structures. In order to calculate structures using AMBER, the first thing that has to be done is locate the charge. For (BK + Na)$^+$ it was placed on the sodium atom. For (BK − H + 2Na)$^+$ it was assumed both sodium atoms possess single positive charges and the carboxyl group at the C-terminus (Arg^9) is deprotonated and carries the negative charge. We considered three possibilities for the location of the charge on (BK + H)$^+$: on Arg^1, on Arg^9, and a zwitter type ion with both Arg^1 and Arg^9 protonated and the carboxyl group on Arg^9 deprotonated. These we will label isomers **I**, **II**, and **III**, respectively.

For each of the five systems, 100 conformations and their energies were determined as described in the Theoretical Methods section. These are given in Figure 5 as scatter plots of energy vs cross section. The five plots are amazingly similar with cross sections varying from ~220 to ~250 Å^2 and relative energies between 0 (most stable) and 30 kcal/mol (least stable). In all cases the most compact structures are the most stable with energy increasing with size. The experimental cross sections are also given on the plots as the cross hatched vertical bars. It is apparent that the most stable 0 K structures predicted by AMBER have cross sections ~10% smaller than experiment for all systems. This point will be addressed shortly.

The procedure we used to generate the 100 structures of each system should statistically sample the low energy portion of the phase space. Consequently, it is instructive to analyze these structures to determine the affinity of the charge site for various electronegative elements on the cationized BK molecules. The results are summarized in a schematic fashion in Figure 6. One point that is very striking from the data in Figure 6 is that both guanidine groups on the two argenine residues are strongly involved in the bonding in a high percentage of the structures for all five isomers. A second aspect that strongly stands out is that four of the backbone carboxyl groups are coordinated to the charge site in all cases, although the identity of the specific carboxyls involved is isomer specific. This global, multiple coordination of the charge sites, especially since Arg^1 and Arg^9 are usually involved, is what leads to the similarities in the scatter plots for the various species.

One interesting feature was observed in the (BK − H + 2Na)$^+$ calculations. In 35 of the 100 structures in the scatter plot, one of the Na$^+$ ions coordinated with both of the guanidine groups on Arg^1 and Arg^9 and only occasionally with the backbone carboxyls, forming a cyclic structure. The other Na$^+$ ion nested in the cavity formed and coordinated primarily with the backbone carboxyls and only occasionally with the guanidine group on Arg^1. In the remaining 65% of the structures one of the sodium ions would coordinate with Arg^1 and the second with Arg^9 and both of them with three of the backbone carboxyls. Unfortunately these two very different isomeric sets were predicted to have similar energies and cross sections even though structurally they are quite distinct.

The lowest energy 0 K structures for each of the five forms of cationized BK are given in Figure 7. For ease of identifica-
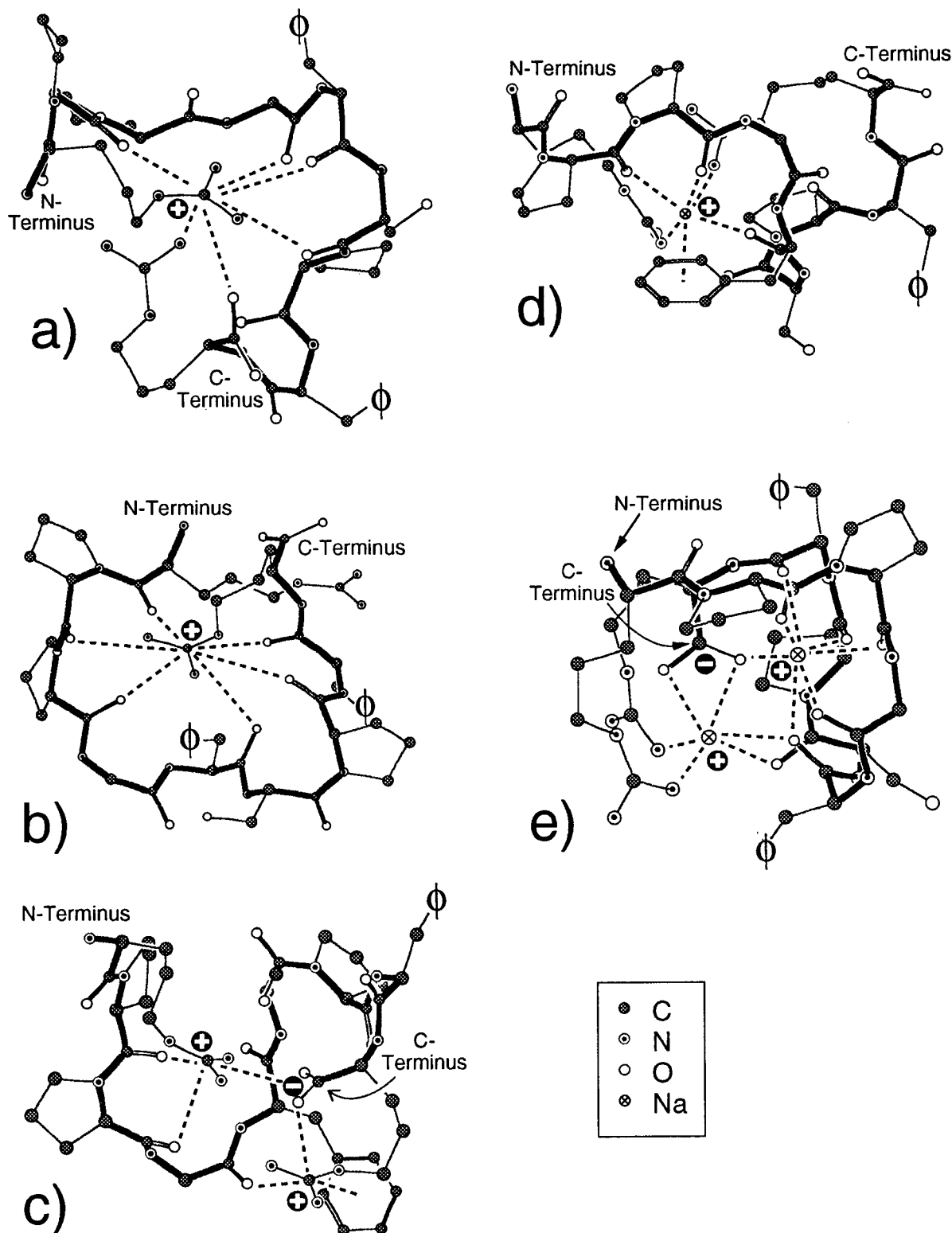
Figure 7. Lowest energy structures of cationized BK. Parts a, b, and c are for isomers **I**, **II**, and **III** of $(BK + H)^+$, part d is for $(BK + Na)^+$, and part e is for $(BK - H + 2Na)^+$. The charge sites are highlighted for ease of identification. The H-atoms are omitted for clarity.

tion large plus signs are given to identify Na^+ ions or sites of protonation and large minus signs for locations of the $-CO_2^-$ group. It is clear that all five systems have very different conformations yet in all cases their cross sections are 220 ± 5 Å^2. The Arg^9 protonated isomer (Figure 7b) has a near circular structure with the N-terminus and C-terminus in close proximity and the charge site near the center of the circle. In each of the other structures the backbone is highly contorted in order to maximize the electrostatic interactions. Among these latter systems the structure of the lowest energy conformer $(BK - H$

$+ 2Na)^+$ is very interesting. The backbone forms a "bobby pin" like structure (Figure 7e) that is then folded in the center to form a taco like cavity that allows good coordination with one of the Na^+ ions. The second Na^+ is remote and coordinates primarily with the guanidine groups of Arg^1 and Arg^9 and both oxygen atoms of the $-CO_2^-$ group. The incredible flexibility of cationized BK demonstrated in these structures is undoubtedly partly responsible for its biological activity, since it can seemingly conform to any shape requirements a receptor site might have.
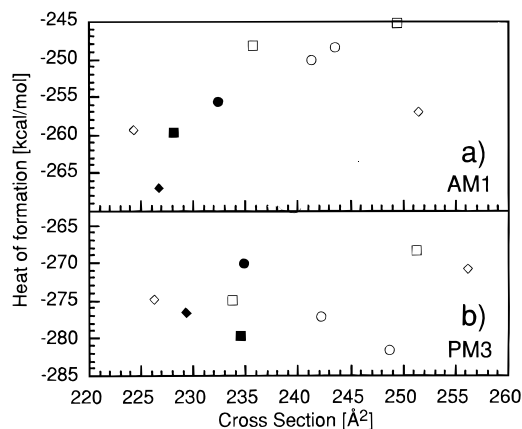
Figure 8. Plot of heat of formation versus cross section for various conformers of $(BK + H)^+$ as calculated by (a) AM1 and (b) PM3 semiemperical calculations. The filled symbols are the lowest energy structures. The initial structures were chosen from the AMBER scatter plots (Figure 5).

While AMBER provides useful relative energies for conformers of a particular cationized form of BK, one cannot compare energies between different cationized forms. Since we could not distinguish the various isomers of $(BK + H)^+$ by their predicted cross sections, we felt it was useful to perform semiemperical quantum calculations on these systems to see if significant differences were observed. These methods have been extensively tested on systems somewhat smaller than those considered here.[17,18] More recently it has been shown that PM3 does a better job than AM1 in dealing with hydrogen bonds and consequently may predict better geometries than AM1. It does in fact yield structures closer to those predicted by ab initio methods in model systems.[55] In a recent study it was shown both methods gave proton affinities of a series of (glycine)$_n$ polymers in good agreement with experiment (to $n = 5$).[56] These authors were able to successfully use PM3 to generate reaction coordinate diagrams that nicely rationalized hydrogen/deuterium exchange in this same set of polymers. Consequently, while molecules the size of BK present a tremendous challenge to these methods in an absolute sense, the very restricted use of them made here seems reasonable.

Since we could not be certain that the AMBER calculations had correctly energy ordered the various conformers within a given isomer, we chose three conformers from each isomer for AM1 and PM3 calculations. Included in each selection was the lowest energy conformer, the lowest energy conformer with a cross section in the experimental range, and a third conformer predicted to have low energy by AMBER. These are designated by the highlighted symbols in the scatter plots (Figure 5). Both AM1 and PM3 calculations were done on these nine conformers and the results summarized in Figure 8. What is apparent in this figure is that all three isomers have about the same energy (± 6 kcal/mol), and the ordering of stability depends on which semiemperical parametrization is used.

One interesting point is the fact the structures calculated by PM3 and AM1 are about 5% less compact than the analagous AMBER structures, as shown in Figure 9, and consequently agree better with experiment. Since these are 0 K structures, any further loosening due to thermal motion should further improve the agreement. At present it is not possible to do "semiemperical" dynamics, but dynamics can be done using AMBER and analogies drawn.

(55) See, for example: Zheng, Y.; Merz, K. M. *J. Comput. Chem.* **1992**, *13*, 1151. Jurema, M. W.; Shields, G. C. *J. Comput. Chem.* **1993**, *14*, 89.
(56) Campbell, S.; Rodgers, M. T.; Marzluff, E. M.; Beauchamp, J. L. *J. Am. Chem. Soc.* **1995**, *117*, 12840.
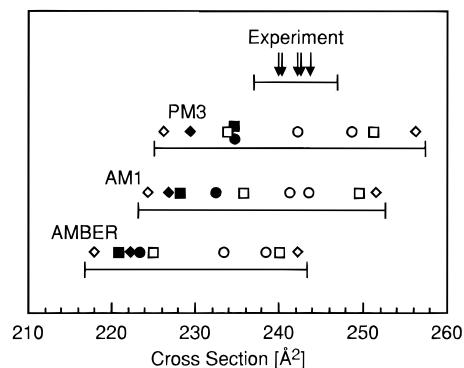

Figure 9. A display of the cross sections for the three conformers of isomers **I**, **II**, and **III** of $(BK + H)^+$ as calculated by AMBER, AM1 and PM3. The spread in experimentally observed cross sections is also shown. The conformers chosen are highlighted in Figures 5 and 8. The filled symbols are the lowest energy AMBER generated conformers.
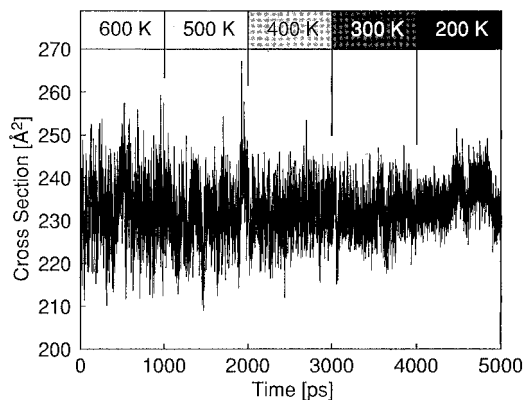

Figure 10. A molecular dynamics run from 600 to 200 K for $(BK + Na)^+$ initiated from the lowest energy AMBER generated conformer. A structure was sampled ever 0.5 ps and its cross section determined. Note the invariance of the average cross section to temperature.

3. Calculated Dynamics. The AMBER suite of programs allows molecular dynamics to be done under constant temperature conditions. We have done so for all five forms of cationized BK as described in the Theoretical Methods section. The results for Arg^9 protonated $(BK + H)^+$ are presented in Figure 10 for successive 1 ns runs at 600, 500, 400, 300, and 200 K. Similar results were obtained for the other four cationized BK ions. What is apparent is that the ions undergo larger conformational excursions as temperature increases (i.e., from ~210 to 260 Å at high temperature and 230 to 240 Å at low temperature), but the average cross section is essentially independent of temperature from 200 to 600 K. This predicted insensitivity of the average cross section to temperature is in agreement with experiment as shown by comparison of Figure 4a with Figure 4b.

Another point worth noting is the average cross section for the thermally averaged conformations increases to ~228 ± 6 Å^2 from 220 ± 5 Å^2 for the 0 K structures, resulting in somewhat better agreement with experiment.

At 200 K, the system occasionally makes a rather large conformational change. Two examples are given in Figure 10. At this lower temperature it takes the system longer to recover than at higher temperatures. The excursions noted in Figure 10 are ~10 Å^2 or 4.3% of the cross section which should be observable if they could be frozen in place for the entire trip through the IC cell (~250 μs). We did experiments down to 80 K but were unable to notice any discernible asymmetries in the arrival time distributions, which should have been apparent
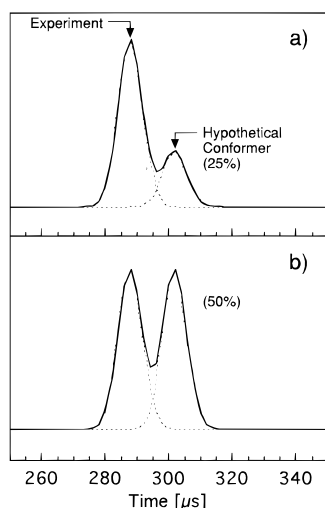
Figure 11. Experimental arrival time distributions for $(BK + H)^+$ at 80 K are given as the peak at shorter times. This peak was convoluted with a peak appropriate for a conformation with 5% greater cross section with 25% abundance (a) and 50% abundance (b). Clearly the two peaks are easily resolved.

if a significant fraction of the ions deviated from the main conformation by 4.3% in cross section (Figure 11).

Discussion

There are a number of important points that can be directly made from the data. The first of these is the fact that no structure is observed in the arrival time distributions of any of the BK systems studied at any temperature (80 to 600 K). Consequently it can be unambiguously concluded that in none of the three systems studied is there a significant fraction of non interconnecting conformers that vary in cross section by more than 2 or 3% (this point will be further amplified later in this section). The AMBER dynamics calculations gave evidence of conformer changes of ~5% in cross section at 200 K (Figure 10) that were relatively long lived (~250 ps), but apparently these conformers were not frozen out even in the 80 K experiments.

A second observation was the lack of temperature dependence of the experimental cross sections from 300 to 600 K (Figure 4). Again this feature was observed for all systems (i.e. H^+ or Na^+ cationized BK). In our earlier work on Na^+ cationized PEG polymers we found the average cross sections increased with temperature as did the structural excursions at a given temperature, and the larger the system the greater the fractional increase.[31] This was interpreted in terms of an electrostatic "core" of oxygen centers bound to the Na^+ ion that had little change in cross section with temperature and a portion of the polymer remote from the charge site that increased its average size with temperature (through dynamical excursions). Consequently, the fact no temperature dependence was observed for any cationized BK systems strongly implies the charge site globally binds the entire peptide through electrostatic interactions.

The AMBER modeling semiquantitatively agrees with both of these observations. The lowest energy 0 K AMBER cross sections for the three $(BK + H)^+$ isomers, the $(BK + Na)^+$ system, and the $(BK - H + 2Na)^+$ system are the same within 2%. Further, the scatter plots of 100 relatively low energy structures are virtually indistinguishable for these rather different systems. The similarities in the cross sections found both experimentally and by AMBER calculations were not anticipated by us. We felt the fact that the proton (or protons) in $(BK +$

$H)^+$ must be localized on Arg^1, Arg^9, or both and that the intramolecular bonding (solvation) of the localized proton would be very different than that of the mobile Na^+ ion would lead to measurably different cross sections for the two systems.

The insensitivity of the cross section to temperature could possibly be due to hot ions exiting the MALDI source that are never thermalized in the high pressure drift cell. We feel this is unlikely for several reasons. First the Na^+ cationized PEG polymers were also made by MALDI in the same source, and they showed significant and reproducible temperature dependence. Second, many annealing experiments[57,58] have been done both in our lab[59] and elsewhere,[60] and all the evidence points to rapid collisional heating and cooling on a time scale short relative to typical ion transit times in the drift cell. Marzluff et al.[61] have unambiguously shown that energy transfer between peptides and small molecules is very efficient. Using their estimates, thermalization of "hot" BK should occur in no more than 1000 collisions, where 25 000 collisions are typical in the IC cell under normal conditions. Hence, the lack of temperature dependence of the experimental cross section is a real effect and must be due to strong, global interactions of the charge site with the entire peptide.

The observed peak widths are slightly broader than those expected from the transport equations of a single species of fixed mobility (Figure 3). This broadening could be due to the presence of a number of conformers with nearly the same mobility that do not easily interconvert. For example, for $(BK + H)^+$ all three isomers might be present and if the intramolecular proton transfer between the isomers is slow relative to the ion drift time, their slightly different cross sections could cause this effect. There cannot, however, be significant contributions to the arrival time distribution from conformers that differ by much more than 2% in cross section. In Figure 11 the experimental peak observed at 80 K for $(BK + H)^+$ is reproduced and convoluted with a peak from an assumed second conformer whose cross section is 5% greater. The 80 K data were chosen because at this temperature both the probability of freezing out different conformers and the experimental resolution are maximized. Data are shown for second conformer probabilities of 0.5 and 0.25. Given the signal to noise available in our experiment we feel a conformer composing 10% of the total BK ions shifted from the main feature by $\geq$3% in cross section would be observable. No such features are observed in any of the three systems reported here.

The question of conformer interconversion and how it depends on temperature is an interesting one and can be explored using AMBER. One useful way to do this is to plot the distance of the charge center from different electronegative sites as a function of time for different temperatures. A sampling of the many such correlations we have obtained is given in Figure 12 for $(BK + Na)^+$. Here the distance of the Na^+ ion to the carbonyl oxygens of four amino acids is given over the temperature range 600 to 200 K. The starting structure was the lowest energy structure given in Figure 7. At 600 and 500

(57) Annealing is effected in ion chromatography by injecting the ion of interest into the IC cell at high energy. The result is rapid collisional heating of the ion, which induces isomerization to occur, followed by collisional cooling and thermalization of the ion. This entire process occurs in the first 5% of the IC cell under typical conditions. This method was developed in Martin Jarrold's lab (ref 58).

(58) Jarrold, M. F.; Horea, E. C. *J. Am. Chem. Soc.* **1992**, *114*, 459.

(59) See, for example: von Helden, G.; Gotts, N. G.; Bowers, M. T. *Nature* **1993**, *363*, 60; *J. Am. Chem. Soc.* **1993**, *115*, 4363; *Chem. Phys. Lett.* **1993**, *212*, 214.

(60) See, for example: Hunter, J.; Fye, J.; Jarrold, M. F. *Science* **1993**, *260*, 784; *J. Phys. Chem.* **1993**, *97*, 3460.

(61) Marzluff, E. M.; Campbell, S.; Rodgers, M. T.; Beauchamp, J. L. *J. Am. Chem. Soc.* **1994**, *116*, 6947.
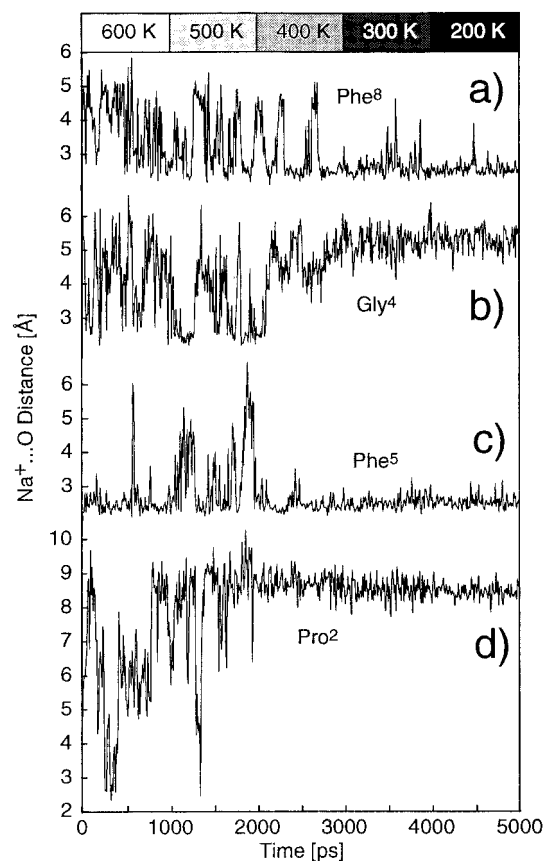
Figure 12. Plot of the distance from Na^+ to various carbonyl oxygens versus time for the temperature range 600 to 200 K. The carbonyl oxygens are shown for (a) Phe^8, (b) Gly^4, (c) Phy^5, and (d) Pro^2. The large distance variations observed at the higher temperatures indicate significant structural variation at these temperatures.

Figure 13. A plot of the distance from the center carbon on the guanidine group of Arg^9 protonated $(BK + H)^+$ to each of the nine carbonyl centers on BK versus time at (a) 80 K. The data in part b were obtained by energy minimization to 0 K structures of the 80 K data.

K large excursions were observed, especially for Pro^2. Some excursions are still observed at 400 K, but by 300 K the system has settled on its basic conformation and only relatively minor conformational changes are observed on the 1 ns time scale, and these changes rapidly revert to the favored conformation. In this particular run the carbonyl on Pro^2 started initially coordinated to the Na^+ ion, but the final conformation has it nearly 9 Å from Na^+. The Na^+ ion has clearly migrated toward the C-terminus and BK has dramatically adjusted its backbone to accommodate this migration. The final structure is not one of the more common ones as evidenced by the correlation data in Figure 6.

Experiments were run as low as 80 K, and a 1 ns dynamics run for Arg^9 protonated $(BK + H)^+$ is given in Figure 13. Again the lowest energy structure shown in Figure 7 was used as the starting point. The results in Figure 13a indicate bond rotations still occur but in no case is the coordination of the charge site to a particular carbonyl oxygen broken. When 0 K structures are obtained from the 80 K data it is clear that a single structure totally dominates. There are occasional minor conformational changes, however, and in these an interesting correlation of structural change is seen throughout the molecule.

Our interpretation of these results is as follows. We see narrow ATD peak widths at all temperatures from 80 to 600 K, only slightly broader than those predicted by the transport equations for a single structure. At 600 K the modeling results seem to require substantial and rapid conformational changes on the μs time scale appropriate for the experiments. Conformational excursions can be large, but these rapidly revert to more stable conformations. This motional averaging gives the appearance of a single structure due to the rapidity of the
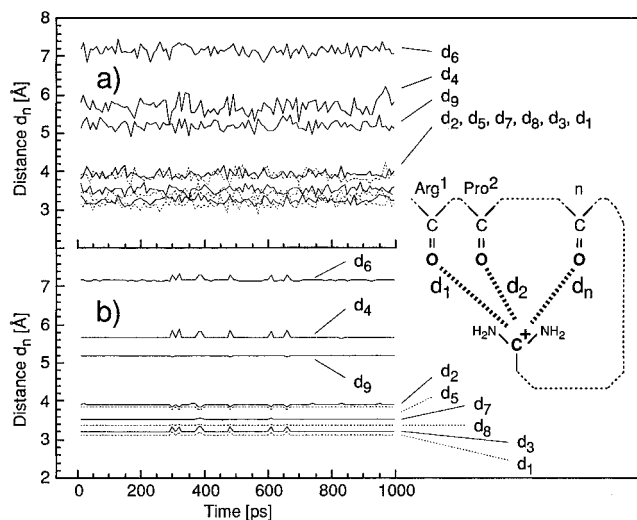
conformational changes. As temperature decreases, the frequency of large conformational excursions rapidly decreases as well. Below 300 K there are probably only a few of the lowest energy conformations present, and these have quite similar, but not identical, cross sections. Once the system becomes trapped in one of these conformations, it is rare if coordination of the charge site with one of the electronegative centers changes, a view consistent with our results on Na^+ cationized PEG polymers. Apparently the reason the cross section does not increase at high temperature is the fact that both expansion and contraction occurs relative to the lowest energy structures and these approximately cancel.

The AMBER 0 K generated cross sections are consistently smaller than experiment by about 10%. When thermal averaging is done using the dynamics simulations this gap narrows but still remains greater than 5% for $(BK + H)^+$ and $(BK + Na)^+$ and only just below 5% for $(BK - H + 2Na)^+$. Semiemperical AM1 and PM3 calculations at 0 K tend to increase the 0 K AMBER cross sections by 4 to 5%. Unfortunately, dynamics cannot be done using AM1 or PM3. However, if these 0 K structures then expand due to thermal motion, as the AMBER structures do, then they would be in quite good agreement with experiment.

One reason AMBER could predict structures that are too compact is an over emphasis in the parametrization of the electrostatic contribution to the binding at the expense of van der Waals interactions. To test this possibility we reduced the charge on Na^+ to 0.5 q and also reduced the partial charges on BK to half of those recommended by AMBER. (We realize changing only a single parameter disrupts the balance built into the AMBER force field but felt such tests could possibly provide insight in parameter improvement.) In this instance the Na^+ ion simply dissociated from the BK molecule at the 800 K temperature used in our annealing method of generating low energy structures. For charge reductions between 0.7 and 0.99 q the Na^+ ion stayed attached to BK at 800 K. A scatter plot was generated for 0.75 q and compared with those given in Figure 5. Somewhat to our surprise there was no discernible difference in the scatter plots. Hence, the 0 K structures show little dependence on the magnitude of the electrostatic interaction.

We have also investigated the effect of charge reduction on the dynamics. The decreased electrostatic binding allows
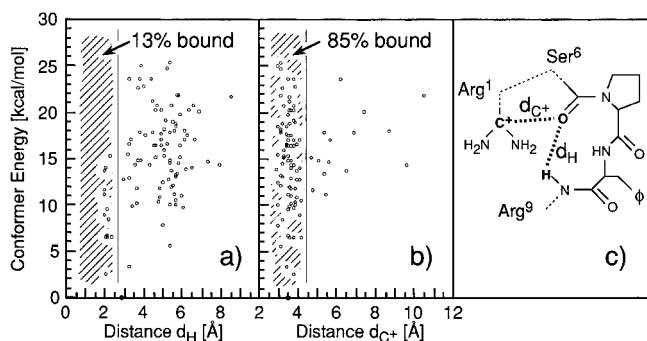
Figure 14. A plot of relative conformer energy versus distance in Arg[1] protonated (BK + H)[+] for (a) the distance from the amide hydrogen on Arg[9] to the carbonyl oxygen on Ser[6] suggesting a β-turn occurs for distances less than 2.5 Å, and (b) the distance from the central carbon on the guanidine group of Arg[1] to the carbonyl oxygen on Ser[6]. The data were obtained from the 100 structures of the scatter plot in Figure 5. The cross hatched regions in parts a and b are where bonding has occurred. A schematic structure is shown in part c.

Table 1. Fraction of β-Turns Observed in AMBER Generated Structures[a]

system		% β-turn
(BK + H)[+]	isomer I[b]	13
(BK + H)[+]	isomer II[c]	1
(BK + H)[+]	isomer III[d]	5
(BK + Na)[+]		6
(BK − H + 2Na)[+]		1

[a] Taken from 100 low energy structures for each system generated by AMBER (Figure 5). [b] Arg[1] protonated BK. [c] Arg[9] protonated BK. [d] Arg[1] and Arg[9] protonated and C-terminus carboxyl group deprotonated.

substantially greater expansive excursions of BK and has less effect on contractive excursions. The net effect is an increase in cross section to about 240 Å[2], in better agreement with experiment. However, there is also a small increase in cross section with temperature (~4% from 200 to 600 K) that is not observed experimentally. Hence, while the electrostatic terms in the AMBER parametrization may be partially responsible for predicting structures of cationized BK that are too compact, it appears a more sophisticated reparametrization will be required to adequately address the problem.

Multiple pulse NMR experiments have been done on BK in water and in sodium dodecyl sulfate.[36] A limited number of dipolar proton correlations were obtained using nuclear Overhauser methods, and an unambiguous structure of BK in these media could not be determined. The authors did feel, however, that analysis of their data using molecular mechanics indicated a β-turn[62] was most likely present between residues Ser[6] to Arg[9] at the C-terminus. The molecular mechanics methods used by Lee et al.[36] suggested the driving force for the β-turn was the hydrogen bond between hydrogen on the amide nitrogen on Arg[9] and the carbonyl oxygen on Ser[6].

While it was not explicitly stated in the paper by Lee et al., presumably their molecular mechanics simulations assumed BK was doubly protonated at Arg[1] and Arg[9]. There was also no mention of the assumed dielectric constant. In a separate paper, Salvino et al.[47] used molecular mechanics annealing methods to generate 100 low energy structures. These structures were compared to those that Lee et al. felt were consistent with their NMR data and some reasonable correlations were found. All calculations of Salvino et al. were done solvent free using a dielectric constant of 1 [although a few calculations for dielectric constants of 4 and 25 were also done but little change was observed]. Presumably both Arg[1] and Arg[9] were protonated in these calculations, but it was not specifically stated. No molecular dynamics was done to assess the role of thermal motion on their structures.

Both Salvino et al.[47] and Lee et al[36] found β-turns to be important, and Salvino et al. state a large percentage of their calculated structures had a β-turn in the Ser[6]-Pro[7]-Phen[8]-Arg[9] sequence at the C-terminus. We have analyzed all 500 of the 0 K minimized structures we generated and only for Arg[1] protonated (BK + H)[+] are a significant number of β-turns observed, and then only 13 out of 100 (Figure 14a). In all other

systems only a few β-turns are observed in the 100 structure sets (Table 1). By contrast, the protonated Arg[1] site correlates with the carbonyl on Ser[6] 85% of the time. These results are in contrast to the conclusions drawn from the solution NMR data and from the molecular mechanics calculations of Salvino et al., presumably both dealing with (BK + 2H)[2+]. We are in the process of expanding our studies to the (BK + 2H)[2+] system to provide a more direct comparison with these earlier results.

Conclusions

Experiments have been done that yield accurate 3-dimensional cross sections of (BK + H)[+], (BK + Na)[+], and (BK − H + 2Na)[+], over the temperature range 80 to 600 K. These results have been analyzed using extensive molecular mechanics and molecular dynamics modeling using the AMBER 4.0 suite of programs. The following are our primary findings:

1. The cross sections of (BK + H)[+], (BK + Na)[+], and (BK − H + 2Na)[+] are all very similar suggesting the polypeptide wraps itself around the charge site in a globular manner.

2. The arrival time distributions are all slightly broader than expected for a single conformer at all temperatures. The implication is that at lowest temperatures (≤200 K) only a few conformers exist with very similar cross sections. At the highest temperatures (≥500 K) rapid conformational change occurs, but it is centered on the conformers of lowest energy.

3. The cross sections are independent of temperature between 300 and 600 K, indicating the charge site interacts globally, holding the molecule into a globular conformation even at highest temperatures.

4. The AMBER cross sections are ~10% smaller than experiment for 0 K structures and ~5% below experiment when thermal averaging is done. Calculations using AM1 and PM3 semiemperical methods give cross sections ~5% larger than AMBER in good agreement with experiment. It appears that the AMBER parametrization needs adjustment to accurately reflect gas phase conformations, but further work needs to be done to verify this.

5. Calculations indicated that the charge site interacts most often with four of the carbonyl oxygens, but which four depends on the specific system. The guanidine groups Arg[1] and Arg[9] are coordinated to the charge site a very high percentage of the time.

6. We found that β-turns at the C-terminus end of the molecule occurred rarely, usually less than 6% of the time. Earlier solution NMR work[36] on (BK + 2H)[2+] indicated β-turns in this region were important, a result consistent with subsequent molecular mechanics studies.[47] Work in our group on (BK + 2H)[2+] in the gas phase is underway to explore this question further.

(62) Perczel, A.; McAllistor, M. A.; Császár, P.; Csizmadia, I. G. *J. Am. Chem. Soc.* **1993**, *115*, 4849 and references therein.